Exploring regulatory functions and enzymatic activities in the nidovirus replicase

Nedialkova, D.D.

Chapter 5

Arterivirus subgenomic mRNA synthesis and virion biogenesis depend on the multifunctional nsp1 autoprotease

Marieke A. Tijms*,
Danny D. Nedialkova*,
Jessika C. Zevenhoven-Dobbe*,
Alexander E. Gorbalenya, and
Eric J. Snijder

*Equal contribution

J. Virol. 2007. 81(19):10496-505
Reprinted with permission

ABSTRACT

Many groups of plus-stranded RNA viruses produce additional, subgenomic mRNAs to regulate the expression of part of their genome. Arteriviruses and coronaviruses (order *Nidovirales*) are unique among plus-stranded RNA viruses for using a mechanism of discontinuous RNA synthesis to produce a nested set of 5′- and 3′-coterminal subgenomic mRNAs, which serve to express the viral structural protein genes. The discontinuous step presumably occurs during minus-strand synthesis and joins noncontiguous sequences copied from the 3′- and 5′-proximal domains of the genomic template. Nidovirus genome amplification ("replication") and subgenomic mRNA synthesis ("transcription") are driven by 13 to 16 nonstructural proteins (nsp's), generated by autocatalytic processing of two large "replicase" polyproteins. Previously, using a replicon system, the N-terminal nsp1 replicase subunit of the arterivirus equine arteritis virus (EAV) was found to be dispensable for replication but crucial for transcription. Using reverse genetics, we have now addressed the role of nsp1 against the background of the complete EAV life cycle. Mutagenesis revealed that nsp1 is in fact a multifunctional regulatory protein. Its papain-like autoprotease domain releases nsp1 from the replicase polyproteins, a cleavage essential for viral RNA synthesis. Several mutations in the putative N-terminal zinc finger domain of nsp1 selectively abolished transcription, while replication was either not affected or even increased. Other nsp1 mutations did not significantly affect either replication or transcription but still dramatically reduced the production of infectious progeny. Thus, nsp1 is involved in at least three consecutive key processes in the EAV life cycle: replicase polyprotein processing, transcription, and virion biogenesis.

INTRODUCTION

The replication of plus-stranded RNA viruses of eukaryotes depends on a unique process of cytoplasmic RNA-dependent RNA synthesis that is primarily directed by an enzyme complex, always including an RNA-dependent RNA polymerase (RdRp), that is produced by translation of the incoming viral genome (reviewed, e.g., in references[1, 3, 7]). The "nonstructural proteins" (nsp's) or "replicase subunits" of mammalian plus-stranded RNA viruses are commonly produced by proteolytic cleavage of larger polyproteins (reviewed e.g., in references[10,14]). This strategy can be supplemented with the synthesis of additional, subgenomic (sg) mRNAs, a process referred to as "transcription" for the purpose of this article, to express additional proteins (reviewed in reference[34]). Members of the order Nidovirales of plus-stranded RNA viruses (*Arteriviridae*, *Coronaviridae*, and *Roniviridae*) rely heavily on the latter strategy (reviewed in references[39, 49,50]) to produce their structural proteins from genes located in the 3'-proximal third of their genome (Fig. 1).

Nidoviruses have been grouped together on the basis of similarities in genome organization and nonstructural and structural protein expression strategies, as well as the presumed immediate common ancestry of key replicative enzymes (see our recent reviews in references[12,56] and references cited therein). The nidovirus replicase/transcriptase, which will be referred to as "replicase" for simplicity, is expressed from the genome RNA by translation of the large open reading frames (ORFs) 1a and 1b (Fig. 1). This yields polyproteins pp1a and pp1ab, with the latter being produced via a conserved ORF1a/ORF1b -1 ribosomal frameshift mechanism (see reference[5] and references cited therein). Nidovirus replicases, in particular those of nidoviruses with large genomes (corona-,toro-, and roniviruses [25 to 31 kb]), include several enzymatic activities that are rare or lacking in other RNA viruses[11, 12, 32, 53, 73]. Triggered by the 2003 outbreak of severe acute respiratory syndrome (SARS)-coronavirus, significant progress has been made in the functional and structural characterization of coronavirus replicative proteins[4, 32, 73]. Still, many questions remain regarding the molecular mechanisms that nidoviruses have evolved to coordinate the various steps of their replicative cycle.

The arterivirus family is the nidovirus branch that stands out for its much smaller genome size (12 to 16 kb). The pp1a and pp1ab replicase polyproteins of the arterivirus prototype equine arteritis virus (EAV)[54] are 1,727 and 3,175 amino acids (aa) long, respectively (for reviews, see references[12, 52, 55]) and are cleaved (Fig. 2A) into 13 nsp's by viral proteases contained in nsp1, nsp2, and nsp4[63, 75]. Seven structural protein genes, residing in the 3'-terminal quarter of the EAV genome, are expressed from a nested set of sg mRNAs (Fig. 1) and are all dispensable for replication and transcription[36].

Nidovirus RNA synthesis in infected cells entails both amplification of the viral genome and sg RNA production. The "bodies" of arteri- and coronavirus sg mRNAs are 3'-coterminal, but they also contain a 5' common leader sequence that is identical to the 5' end of the genome. Replication and transcription are thought to proceed through different minus-strand intermediates. Whereas a full-length minus-strand template is used for replication, sg mRNAs are assumed to be synthesized from subgenome-length minus

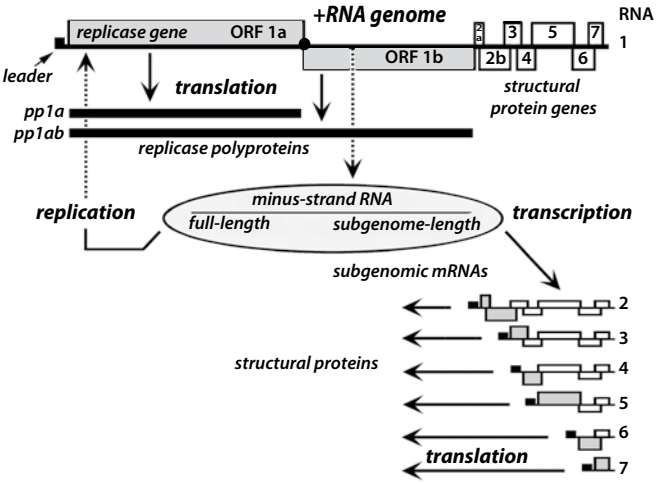

Figure 1. Schematic diagram of the genome organization and expression of EAV**.** The regions encoding the replicase polyproteins (pp1a and pp1ab) and structural proteins are indicated on the genome. The replication/transcription complex, presumably containing the full-length and subgenome-length minus-strand templates for replication and transcription, is depicted below the genome. Subgenomic mRNAs, with the black boxes representing their common 5′ leader sequence, are shown in the bottom part of the scheme.

strands, generated by a process of discontinuous RNA synthesis (reviewed in references[39, 48–50, 70]) involving the 3′-terminal extension of the nascent strands (the complements of the sg mRNA bodies) with the complement of the leader sequence. This discontinuous step in minus-strand RNA synthesis, which may resemble copy-choice RNA recombination, is regulated (in part) by conserved transcription-regulating sequences (TRSs). In EAV, both sequence elements and higher-order RNA structures have been postulated to direct the transfer of the nascent minus strand from the body TRS to the leader TRS in the genomic RNA template[38, 40, 41, 64, 65]. In addition to these RNA-RNA interactions, several EAV replicase subunits have been specifically implicated in transcription: the nsp10 helicase[51, 68, 69], the nsp11 putative endoribonuclease[45], and nsp1[62], the most N-terminal replicase cleavage product. Previous studies showed that EAV replication can proceed in the absence of transcription[62, 68], suggesting that the latter process is in part controlled by transcription-specific replicase functions. Whereas mutations in nsp10 and nsp11 affected both genome amplification and transcription[45, 68], deletion of the nsp1-coding sequence from the replicase gene selectively blocked sg RNA synthesis[62], which could be partially restored in a replicon RNA that expressed nsp1 from an artificial alternative locus in the genome (replicon DITRAC)[62]. EAV nsp1 (260 aa) cotranslationally releases itself from the replicase polyproteins through a papain-like cysteine protease (PCPβ) activity in its C-terminal half[58, 59]. Comparative sequence analysis identified two other domains in nsp1 (Fig. 2C), an additional PCP (PCPα), which has become inactivated in the course of EAV evolution but is functional in other arteriviruses[9], and a potential N-terminal zinc finger (ZF) domain (Fig. 2B)[62]. In the artificial setting of the DITRAC replicon, the ZF domain and

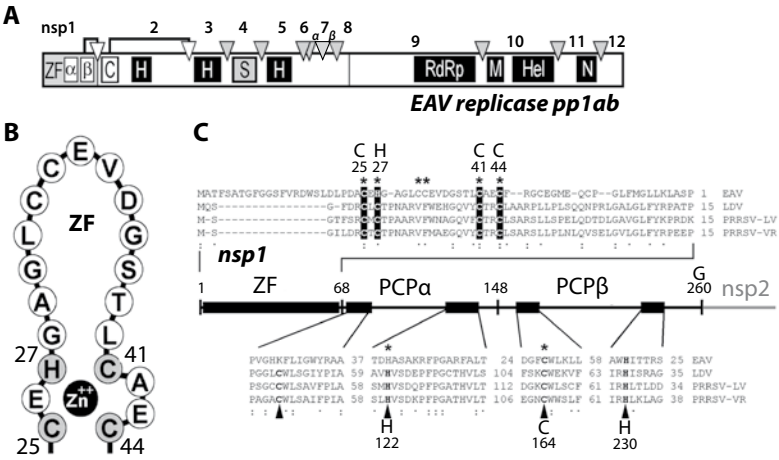

Figure 2. (A) Processing scheme of the EAV replicase, depicted in the form of the pp1ab polyprotein. The three viral protease domains (the nsp1 PCPβ [β], the nsp2 cysteine proteinase [CP], and the nsp4 serine proteinase [S]) and their cleavage sites are indicated. Other domain abbreviations are as follows: ZF, nsp1 zinc finger domain; α, nsp1 PCPα domain; H, hydrophobic domains; RdRp, RNA-dependent RNA polymerase (nsp9); M, metal-binding domain (nsp10); Hel, helicase (nsp10); N, nidovirus-specific endoribonuclease NendoU (nsp11). (B) Schematic representation of the putative nsp1 ZF domain, showing the four residues that are proposed to coordinate zinc in gray. (C) Comparison of key sequences of the three domains identified in the arterivirus nsp1 region, ZF, PCPα, and PCPβ. The putative zinc-coordinating residues of the ZF domain and the active-site Cys and His residues of the two PCP domains are indicated. Note that EAV PCPα is no longer active due to the loss of its active-site Cys (9). Residues targeted by mutagenesis in this study are indicated with an asterisk.

the structural integrity of nsp1, but not the proteolytic activity of PCPβ, were important for transcription[62]. The role of nsp1 has now been addressed in the context of the full-length EAV genome and the complete viral life cycle. We conclude that EAV nsp1 not only couples replicase maturation to transcription but also plays a surprising, yet unexplained, role in virion biogenesis. Several nsp1 mutations that did not dramatically affect viral RNA synthesis were found to severely reduce the production of infectious progeny. Thus, EAV nsp1 is a multifunctional protein that is involved in at least three consecutive key processes in the EAV life cycle: proteolytic maturation of the replicase, transcription, and virion biogenesis.

MATERIALS AND METHODS

EAV reverse genetics

Site-directed PCR mutagenesis[25] was used to engineer mutations in shuttle plasmids carrying the nsp1 coding sequence. Following sequence analysis, mutations were transferred to EAV full-length cDNA clone pEAV211[64, 68]. The mutants of the PCPβ active-site cysteine

(Cys-164) and the nsp1/2 cleavage site (Gly-260/Gly-261) have been described before[58]. The amino acid substitutions engineered to generate novel nsp1 mutants are listed in Table 1.

Following *in vitro* transcription of full-length cDNA clones by T7 RNA polymerase, BHK-21 cells were transfected with equal amounts of full-length EAV RNA as described previously[68]. Immunofluorescence assays (IFAs)[67, 68] were used to monitor transfection efficiencies.

Analysis of virus mutants

For an initial assessment of viral phenotypes (in terms of replication and transcription), dual-labeling IFAs[67] were performed with a rabbit antiserum specific for nsp3[43], a replicase cleavage product expressed from the genome, and a mouse monoclonal antibody (MAb) recognizing the nucleocapsid (N) protein (N MAb 3E2)[29], which is expressed from the smallest sg mRNA. Viral RNA synthesis was studied in more detail by isolating total intracellular RNA at the end of the first replication cycle (~14 h post-transfection [hpt]) using the acidic phenol extraction method, as described previously[70]. RNA was separated in denaturing formaldehyde-agarose gels, and viral mRNAs were visualized by hybridization with a radioactively labeled, antisense oligonucleotide probe (complementary to the 3′ end of the genome), which recognizes both genomic and all sg mRNAs[70]. Supernatants harvested from transfected cell cultures were analyzed for infectious progeny by plaque assays[36] and infection of fresh BHK-21 cells.

PCPβ activity assay

A vector (pEAVΔH) for testing PCPβ activity in an *in vitro* transcription and translation assay[58] was engineered by making an internal HindIII deletion (removing nucleotides [nt] 1506 to 12308 of the EAV genome; NCBI accession no. NC_002532) in the full-length cDNA clones for selected mutants. These constructs contained an in-frame fusion of the 5′ end of ORF1a to the 3′ end of ORF6 and encoded a product of 453 aa (52 kDa) including the full-length nsp1 and the nsp1/2 cleavage site. The fusion gene was preceded by a T7 promoter and the natural genomic 5′-untranslated region and followed by the genomic 3′-untranslated region and a poly(A) tail. The *in vitro* PCP assay was performed by translation of transcripts derived from these vectors in a rabbit reticulocyte lysate (Promega). The reaction was performed at 30°C for 90 min in the presence of [^{35}S]methionine, after which translation and cleavage products were analyzed by sodium dodecyl sulfate-polyacrylamide gel electrophoresis (SDS-PAGE) and autoradiography.

Sequence analysis and RNA structure prediction

The RNA structure of the 5′-proximal region of EAV ORF1a was predicted using the genetic algorithm of STAR v4.4[19] and the Zuker algorithm[77] on the M-fold web server[78]. Sequence alignments were created using the ClustalW algorithm incorporated in Vector NTI (Invitrogen). The hairpin structure predicted to underlie the ZF-coding region (see

Fig. 6) was mutated in full-length cDNA clone pEAV211-RNAko using a combination of seven translationally silent mutations in codons specifying residues 22 to 28 of nsp1 (Fig. 6): C-290→A, C-293→U, U-296→A,U-299→C, G-302→A, U-305→C, and C-308→G (numbers refer to positions in the EAV genome sequence).

RESULTS

Design and characterization of EAV nsp1 mutants

We have previously reported that nsp1 is dispensable for EAV genome replication but absolutely required for transcription[62]. In that study, expression of an engineered wild-type nsp1 cassette from an artificial internal ribosomal entry site (IRES) inserted in the 3'-terminal part of replicon DITRAC could complement for the deletion of the natural nsp1-coding sequence from the replicase gene[62]. This resulted in partial restoration of transcription, but since the IRES-nsp1 cassette in the DITRAC replicon replaced five of the seven structural protein genes, virus production could not be studied in this system. To address the role of nsp1 against the background of the complete EAV life cycle, we have now used a reverse-genetics approach based on the use of full-length cDNA clones[68]. Full-length RNA derived from cDNA clones containing nsp1 mutations (Table 1) was transfected into BHK-21 cells. Replication and transcription were initially monitored using a previously described dual-labeling IFA[62] detecting nonstructural and structural protein expression (data not shown). Subsequently, additional assays were used to characterize the phenotypes. The production of infectious progeny was investigated by monitoring the spread of the infection in transfected cell cultures and/or using cell culture supernatants to infect fresh cells.

The nsp1/2 cleavage is essential for EAV genome replication

We first analyzed the importance of cleavage of the nsp1/2 site by the C-terminal PCPβ domain of nsp1[58]. In the setting of the DITRAC replicon, PCPβ activity was dispensable for the functionality of nsp1 in transcription[62]. However, in DITRAC, nsp1 was expressed from a separate IRES-driven cistron and did not have to play its usual role in replicase proteolysis. In this replicon, cleavage of the nsp1/2 bond was effectively substituted for by translation initiation at the 5' end of the nsp2 coding sequence and independent expression of nsp1 from the 3'-proximal part of the genome.

Using a full-length cDNA clone, cleavage of the nsp1/2 site was now found to be a prerequisite for EAV RNA synthesis. Several mutations that were previously reported to abolish processing of the nsp1/2 site[58, 59] rendered the viral RNA noninfectious. These included replacement of the PCPβ active-site Cys-164 with Ser and replacement of the P1 (Gly-260) or P1' (Gly-261) residues of the nsp1/2 cleavage site with Val (Table 1) (data not shown). The lethal effect of these mutations was evident, in several independent experiments, from the complete lack of IFA signal in transfected cells and the absence of viral RNA synthesis and infectious progeny.

Table 1. Overview of the genotype and first-cycle phenotype of EAV nsp1 mutants used in this study

		Codon[a]						
Construct	Mutation	Wild type	Mutant	Replication[b]	Transcription[b]	Plaque size	Titer (PFU/ml)[c]	Phenotype summary[d]
pEAV211	NA[e]	NA	NA	Normal	Normal	Normal	10^7-10^8	Wild-type control
C25A	Cys -25→Ala	UGU	**GC**U	Enhanced	Negative	No plaques	<2x10^1	Transcription negative; nonviable
C25H	Cys -25→His	UGU	**CA**U	Normal	Normal	Small	10^5-10^6	Transcription ~normal; attenuated
H27A	His-27→Ala	CAU	**GCC**	Normal	Normal	Small	10^2-10^3	Transcription ~normal; attenuated
H27C	His-27→Cys	CAU	**UG**U	Normal	Normal	Small	10^2-10^3	Transcription ~normal; attenuated
H27R	His-27→Arg	CAU	C**G**U	Enhanced	Reduced	Normal	10^2-10^3	Transcription impaired; rapid reversion
C32A C33A	Cys -32→Ala Cys -33→Ala	UGC UGC	**GCG** **GC**C	Normal	Normal	Normal	10^7-10^8	Wild type
C41A	Cys -41→Ala	UGC	**GCG**	Enhanced	Negative	No plaques	<2x10^1	Transcription negative; nonviable
C41H	Cys -41→His	UGC	**CAU**	Enhanced	Negative	No plaques	<2x10^1	Transcription negative; nonviable
C44A	Cys -44→Ala	UGU	**GC**U	Enhanced	Negative	No plaques	<2x10^1	Transcription negative; nonviable
C44H	Cys -44→His	UGU	**CA**U	Enhanced	Negative	No plaques	<2x10^1	Transcription negative; nonviable
C164S	Cys-164→Ser	UGC	**A**GC	Negative	Negative	No plaques	<2x10^1	Replication negative; nonviable
G260V	Gly-260→Val	GGC	G**UA**	Negative	Negative	No plaques	<2x10^1	Replication negative; nonviable
G261V	Gly-261→Val	GGC	G**UA**	Negative	Negative	No plaques	<2x10^1	Replication negative; nonviable
RNAko	7 silent mutations	See text	See text	Normal	Normal	Normal	10^7-10^8	Wild type

[a] Nucleotide substitutions are indicated in boldface.
[b] Transfected cells were analyzed by IFA and Northern blot analysis at the end of the first cycle of replication (14 to 16 hpt).
[c] Infectious progeny titers in plaque assays of medium from transfected cells harvested at 18 hpt.
[d] Depending on the mutant, data from two to four independent transfection experiments are summarized.
[e] NA, not applicable.

These results are in contrast with our previous observation that deletion of nsp1 selectively blocks transcription but not replication[62]. We therefore conclude that cleavage of the nsp1/2 site by the nsp1 PCPβ domain must be essential to produce a functional EAV replication complex. Possibly, the N terminus of nsp2 has to be liberated for this subunit to fulfill its role in the formation of the membrane-bound replication complex[43, 57]. This

interpretation is further supported by the nonviable phenotype of an EAV construct, in which green fluorescent protein (GFP) was fused to the N terminus of nsp2[66].

The nsp1 ZF domain plays a critical role in transcription

On the basis of site-directed mutagenesis of Cys-25 and Cys-44 (both residues changed to Ala) in the DITRAC replicon, the nsp1 ZF domain was previously implicated in regulation of transcription[62]. In the context of the EAV full-length clone, the ZF domain was now probed more extensively (Table 1). The four putative zinc-coordinating residues (Cys-25, His-27, Cys-41, and Cys-44) were targeted, and - as a negative control - two Cys residues (Cys-32 and Cys-33) that are not conserved in arterivirus nsp1 sequences (Fig. 2C) were also replaced. Nonconservative mutagenesis (to Ala) of the latter two residues resulted in a wild-type phenotype, indicating that Cys residues at positions 32 and 33 of the EAV ZF domain are dispensable for replication in cell culture. The four putative zinc-coordinating residues were replaced both nonconservatively (Cys or His to Ala or Arg) and conservatively (Cys to His and His to Cys). The latter strategy was aimed at maintaining (partial)

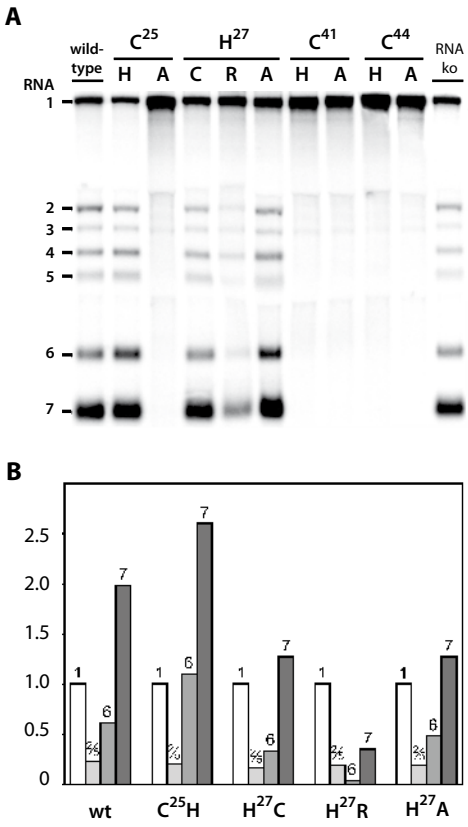

Figure 3. (A) Northern blot analysis of genome (RNA1) and sg mRNA (RNAs 2 to 7) synthesis in BHK-21 cells transfected with EAV nsp1 ZF mutants (14 hpt) and the RNAko mutant designed to probe the role of the RNA structure of the ZF-coding region (see text). RNA was isolated at 14 hpt, and hybridization was carried out using a ^{32}P-labeled oligonucleotide probe complementary to the 3′ end of the genome and thus recognizing all viral mRNA species. Note the upregulation of genome synthesis in transcription-negative mutants. (B) Phosphorimager analysis of the ratio of sg mRNA to genome accumulation, based on the gel depicted in panel A. For the transcription-positive mutants, the amount of genome was put at 1 and the relative amounts measured for mRNA7, mRNA6, and mRNAs 2 to 5 are shown. With the exception of the His-27→Arg mutant, all mutants were concluded to maintain fairly normal transcription levels. wt, wild type.

zinc-binding activity. Interestingly, a differential effect of the Ala/Arg versus His/Cys ZF mutations was indeed observed at some positions (Table 1).

Residues Cys-41 and Cys-44 were both absolutely required for the function of nsp1 in transcription (Fig. 3 and Table 1), since their replacement essentially exerted the same effect as deletion of nsp1: transcription was reduced to a level that could not even be detected by using reverse transcription-PCR (RT-PCR) (data not shown). Remarkably, these transcription-negative mutants also displayed a clear upregulation (2.5- to 3-fold) of genome replication (Fig. 3A), suggesting that EAV replication and transcription normally compete for common factors.

Multiple nsp1 ZF domain mutants are transcription positive but severely impaired in virus production

In terms of transcription, the role of Cys-25 was found to be somewhat less critical than those of Cys-41 and Cys-44. Northern blot analysis revealed that the Cys-25→His mutant produced approximately normal amounts of sg mRNAs (Fig. 3B), although replacement with Ala completely eliminated transcription. Immunoprecipitation analyses and IFAs (D. D. Nedialkova et al., unpublished data) confirmed the synthesis of several structural proteins. Remarkably, however, progeny titers were 100- to 1,000-fold reduced and mutant C25H displayed a small-plaque phenotype (Fig. 4).

Replacement of the fourth putative zinc-coordinating residue, His-27, with either Ala or Cys also yielded a transcription-positive phenotype (Fig. 3). sg RNA synthesis appeared somewhat reduced relative to genome synthesis but not more than twofold (Fig. 3B). However, the drop in infectivity for these two His-27 mutants was more pronounced (4 to 5 logs). Signs of probable reversion were occasionally observed in the form of larger plaques (Fig. 4). The His-27→Arg mutant, on the other hand, displayed a clear transcrip-

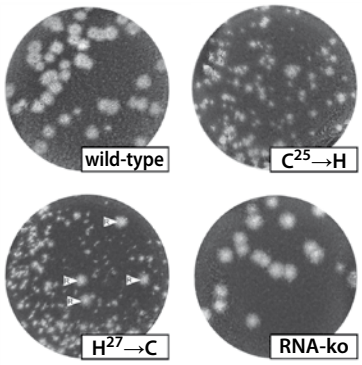

Figure 4. Plaque phenotype of selected mutants from this study. Virus was harvested from transfected BHK-21 cells at 18 hpt. Plaque assays were also performed on BHK-21 cells and fixed after 3 days. The small-plaque phenotype of the Cys-25→His and His-27→Cys mutants is illustrated, with the latter showing sign of probable rapid reversion (plaques marked R). The fourth photograph illustrates the wild-type plaque phenotype of the RNAko mutant.

tion defect (Fig. 3A and B). Some infectious progeny were produced, but in view of their wild-type size, these plaques likely resulted from rapid reversion of the single-nucleotide mutation introduced to create the H27R mutant. All other mutants in our data set required two replacements to revert to the wild-type codon (Table 1), and they were, accordingly, relatively stable.

The characterization of the transcription-positive nsp1 mutants was extended to several other time points after transfection (between 11 and 18 hpt) with essentially identical results, indicating that these mutants are not merely delayed in terms of virus production but fail to produce the normal level of infectious progeny—an observation implicating nsp1 in an additional step of the viral life cycle, downstream of transcription. Analysis of this phenotype in a longer-time-course experiment was complicated by the emergence and spread of revertants, an issue that will be addressed in a follow-up study.

PCPβ proteolytic activity is not affected by mutations in the ZF domain

In view of the critical importance of cleavage at the nsp1/2 site for virus viability (see above), we selected a number of ZF mutants to investigate whether their nsp1 PCPβ activity might have been compromised. PCPβ was previously shown to be highly efficient in directing the nsp1/2 cleavage in a rabbit reticulocyte lysate-based *in vitro* translation system[58]. By making an internal deletion in the full-length cDNA clones for these mutants, we engineered a vector (pEAVΔH) for *in vitro* transcription and translation. The pEAVΔH product was a 52-kDa (453-aa) fusion protein consisting of the full-length nsp1, the N-terminal part of nsp2, and the C-terminal part of the M protein, which is encoded by ORF6.

In vitro transcripts derived from these vectors were translated in a reticulocyte lysate in the presence of [^{35}S]methionine. Reaction products were analyzed directly by SDS-PAGE and autoradiography (Fig. 5). Wild-type nsp1 showed complete cleavage of the 52-kDa precursor into nsp1 (30 kDa) and the C-terminal 22-kDa fragment. The same observation was made for nsp1 ZF mutants showing (C25H and H27C) or completely lacking (C25A and C41A) sg RNA synthesis, strongly suggesting that the transcription defect in the latter mutants is unrelated to a change in PCPβ proteolytic activity.

Analysis of RNA structure of the nsp1 ZF-coding region

The 5′-proximal domain of the arterivirus genome is a multifunctional region containing RNA signals that are known to be involved in translation, replication, and transcription. These signals were previously found to extend into the coding part of the genome, more specifically the 5′ end of ORF1a[64, 65]. This raised the possibility that defects observed in our nsp1 ZF mutants could be due to the effect of the introduced mutations on RNA sequence or structure, rather than on the nsp1 amino acid sequence. In particular, such RNA-specific effects might explain transcription defects, in view of the proximity of the leader TRS and leader TRS hairpin[64, 65]. Also, the production of progeny virus might be

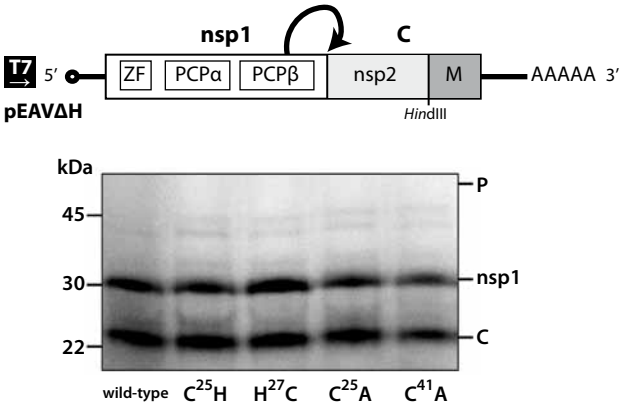

Figure 5. In vitro assay for PCPβ activity in nsp1 ZF mutants. Expression construct pEAVΔH (see Materials and Methods) was used to *in vitro* translate an nsp1-containing fusion protein in the presence of [^{35}S]methionine. Reaction products were analyzed by SDS-PAGE and autoradiography. Cleavage of the 52-kDa precursor (P) yields nsp1 and a 22-kDa C-terminal fragment (C). All nsp1 ZF mutants tested showed wild-type nsp1 PCPβ activity, thus ruling out that a defect in nsp1/2 cleavage was the basis for their phenotype.

affected at the level of genome packaging. The location of encapsidation signal(s) in the EAV genome is still unknown, but previous studies with defective interfering RNAs implicated sequences in the first ~600 nt of the genome in RNA packaging[35].

A comparative analysis of the ZF-coding sequence (nt 285 to 360) of a number of EAV isolates revealed that this area is highly conserved (Fig. 6A). RNA structure predictions using different methods (see Materials and Methods) revealed a prominent and potentially stable hairpin structure (predicted ΔG using Mfold is -13.6 kcal/mol [Fig. 6B]), which can be formed by nt 285 to 315 of the EAV genome. These nucleotides specify nsp1 aa 22 to 30, thus including key ZF residues Cys-25 and His-27, for which mutagenesis had yielded remarkably variable results (see above). Strikingly, the comparative sequence analysis in Fig. 6A provided some additional support for this structure, since four variations found in this region were predicted either to maintain the predicted structure (Fig. 6B; C-293→U and U296→C), to not affect it due to their position in a bulge (A-292→C and U305→C), or to immediately flank the predicted hairpin (A-314→U and U315→C).

In order to address the question whether the defects observed for (some) nsp1 mutants might be due to an effect on the predicted hairpin rather than the nsp1 protein, we engineered a mutant (RNAko) in which a combination of seven translationally silent mutations was introduced in the codons specifying nsp1 residues 22 to 28 (Fig. 6B). Mfold analysis indicated that this combination of mutations in the region of nt 290 to 308 should destroy the predicted hairpin (data not shown). Also some alternative RNA structures that can be predicted for the wild-type sequence would be significantly altered by this combination of mutations. Nevertheless, in multiple experiments, the phenotype of the RNAko mutant was found to be identical to that of wild-type virus, showing normal levels of replication and transcription (Fig. 3), wild-type virus titers (Table 1), and a normal

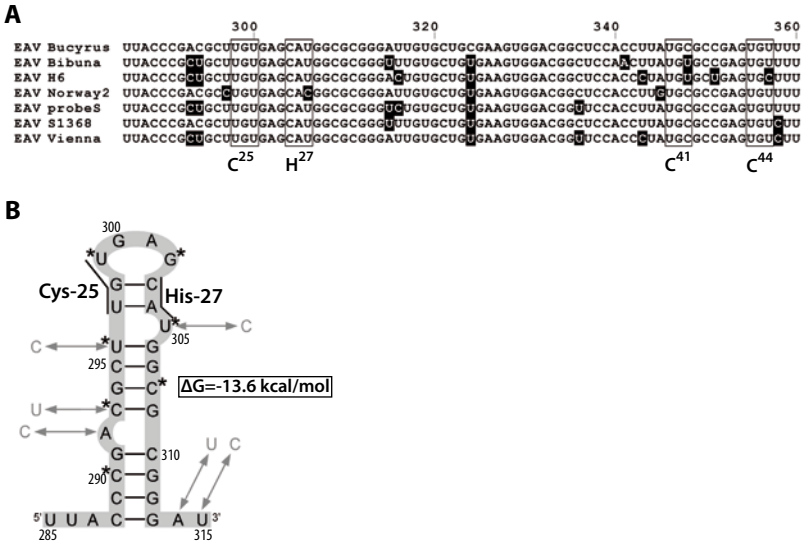

Figure 6. (A) Sequence alignment of the nsp1 ZF-coding domain for a selection of EAV isolates (for details, see reference[64]). The codons for the four key residues of the nsp1 ZF are boxed. (B) Structure of a predicted RNA hairpin that can be formed by the sequence specifying nsp1 ZF residues 22 to 28, thus including the highlighted codons for Cys-25 and His-27. Natural sequence variations (see panel A) are indicated in gray. Residues targeted for mutagenesis in the RNAko mutant (see text) are indicated with asterisks.

plaque size (Fig. 4). Thus, regardless whether the hairpin depicted in Fig. 6 exists or not, it is irrelevant in the context of the results obtained with the Cys-25 and His-27 nsp1 ZF mutants. In this light, also the phenotype of the H27R mutant is important, since its A-304→G mutation is predicted to maintain the RNA hairpin, exchanging a U-A for a U-G base pair. Still, H27R transcription is seriously affected (Fig. 3), again suggesting that it is the nsp1 amino acid sequence that is important rather than the RNA structure of this region.

DISCUSSION

Following uncoating, plus-strand RNA virus genomes are first translated by host ribosomes to produce the enzymes required for viral RNA synthesis. nsp1 of EAV is the first viral protein expressed and thus seems to occupy a strategic position in the viral life cycle, which may explain the multifunctionality of this replicase subunit that is now emerging. In addition to its critical role in replicase polyprotein processing and sg RNA production described before[62] and extended here, our new data implicate nsp1 in an as-yet-undefined function downstream of RNA synthesis that is ultimately important for virion biogenesis.

The data presented in this article, in particular those obtained from mutagenesis of the putative zinc-binding residues of the ZF domain, confirm the crucial role of nsp1 in

EAV transcription. However, whereas EAV proved to be highly sensitive to replacement of Cys-41 and Cys-44, the Cys-25→His substitution was tolerated and the constraints on the His occupying position 27 appeared to be even more relaxed. The fact that - compared to the distal pair of Zn-binding residues (Cys-41 and Cys-44) - mutations at the proximal Cys-25/His-27 pair were relatively well tolerated correlates with (and supports) the alignment presented in Fig. 2C, which shows that the position of His-27 is occupied by Cys in other arteriviruses.

Zinc binding by the nsp1 ZF domain remains to be verified, an issue currently pursued by purification and characterization of recombinant nsp1 from *Escherichia coli*. Also, we cannot formally exclude the theoretical possibility that this region of nsp1 contains, e.g., two small adjacent (or even overlapping) domains with different functions. However, the results obtained upon mutagenesis of the four putative zinc-coordinating residues lend credibility to the hypothesis that they are part of a single ZF domain: e.g., mutations in either pair of proposed zinc-binding residues can produce the same transcription-negative phenotype (compare C25A with the C41/C44 mutants [Fig. 3]). The three transcription-positive ZF mutants (C25H, H27C, and H27A) were also the basis for a second important observation, which was that nsp1 mutations can result in a major defect in the production of infectious progeny, thus implicating the protein in an additional step of the viral life cycle, downstream of transcription. The wild-type phenotype of the RNAko mutant (Fig. 6) makes it highly unlikely that disruption of RNA structures in the nsp1 ZF-coding region played a role in the mixed phenotypes that were observed.

Zinc finger domains are short, independently folded stretches of amino acids that require the coordination of one or more zinc atoms to stabilize their higher-order structure[24]. These motifs were first identified in TFIIIA of *Xenopus laevis* and were implicated in nucleic acid recognition[33]. Since then, ZF domains have emerged as one of the most prevalent motifs in the mammalian proteome. They are frequently classified according to the sequential nature of the zinc-coordinating residues, with the CCHH class being the most common one. ZF domains are widely recognized as sequence-specific DNA-binding motifs, but they have also been shown to bind RNA[28], as well as to participate in protein-protein interactions[27, 30], including dimerization[31]. Given the versatility and diversity of this structural motif, it is not surprising that many viruses also encode ZF proteins. One of the best-characterized examples is the nucleocapsid (NC) protein of onco- and lentiviruses, which contains one or two copies of a CCHC zinc-coordinating domain that is essential for RNA packaging during virus assembly[8, 31]. Upon conservative replacement of zinc-binding residues, zinc coordination is maintained and viral genome packaging is not affected, but the resulting mutant viruses are almost completely noninfectious[15, 16]. Further analysis implicated these ZF domains in viral RNA synthesis and RNA-protein interactions, thus revealing additional, previously unknown functions of these domains[16, 20, 26]. Interestingly, a structural study of zinc fingers of the CCHC type in lentiviruses showed that an HCHC mutant was no longer able to bind zinc tetrahedrally, while the CCHH form could still bind zinc tightly, although this resulted in important structural modifications that could be responsible for the loss of infectivity observed for this mutant[47].

Despite clear differences in protein function and origin, intriguing parallels can be drawn between these retrovirus NC data and our analysis of EAV nsp1 mutants in which putative zinc-coordinating residues were replaced. The transcription-negative phenotype of the Cys-25→A and Cys-41/Cys-44 mutants suggests a complete loss of zinc coordination. However, the conservative replacements of Cys-25→His and His-27→Cys, which in theory may leave the zinc-coordinating potential intact, were both largely tolerated in terms of sg RNA production (Fig. 3), although these mutants were significantly impaired in a later stage of the viral life cycle, possibly virion biogenesis. The His-27→Ala replacement might represent an intermediate that is still able to bind zinc, as described for the distal ZF of the HIV-1 NC (61), in which the same mutant was concluded to retain the tetrahedral coordination of the metal ion, with the vacant ligand position presumably occupied by a water molecule. A similar situation has been described for the CCCH ZF domain in another viral protease, NS3 of hepatitis C virus[22].

Very little is currently known about the protein-protein and protein-RNA interactions that regulate arterivirus sg RNA synthesis. nsp1 might be involved in the stalling of the viral RdRp complex at the body TRSs by interacting with this conserved RNA sequence. It could also participate in the targeting of the nascent subgenome-length minus strand to the leader TRS in the 5′ end of the template or may facilitate the base pairing between body TRS complement and leader TRS - steps that are presumed essential for arterivirus sg RNA synthesis. Regardless of the molecular basis of nsp1 involvement in EAV transcription, the integrity of the ZF domain was also found to be essential for virus production.

Obviously, in the arterivirus system (Fig. 1), structural protein synthesis and consequently virus production are directly controlled by sg mRNA synthesis. It should also be noted that EAV assembly involves a total of seven structural proteins, which are all essential for the production of infectious progeny[36, 71, 72], and that little is known about the molecular interactions between these components and the kinetics of virus assembly. In other words, a small disturbance at the level of sg mRNA synthesis (e.g., affecting the ratio at which some of the structural proteins are produced) could in theory have major consequences for virus production. Still, three of our mutants (C25H, H27C, and H27A) coupled a deviation of not more than twofold in the ratio of genome to sg mRNA synthesis to a 2- to 5-log drop in infectious progeny titers (Table 1). We consider it highly unlikely, but not impossible, that this is solely due to relatively minor changes at the level of sg mRNA production. On the other hand, ostensibly supporting a direct role of nsp1 in virion biogenesis, there are precedents both for the presence of replicase proteins of plus-strand RNA viruses in virions[37, 42, 46] and for a link between mutations in replicase subunits and the production of infectious progeny[23].

A role of nsp1 in translation of viral RNA also needs to be investigated, although a preliminary analysis did not reveal major deviations in structural protein synthesis for mutants like C25H (D. D. Nedialkova et al., unpublished data). As in the case of the function of nsp1 in transcription, a better understanding of this phenotype and the role of nsp1 will require identification of interaction partners, which may be either RNA sequences or

other viral proteins. Such studies are currently ongoing using biochemical methods and attempting to isolate second-site revertants for selected nsp1 mutants.

Finally, the data in this paper underlines the importance of the nsp1 PCPβ domain in the EAV system. This enzyme is a representative of a class of papain-like "accessory proteases" (a term used to discriminate them from the viral "main" protease), which are found in evolutionarily distinct lineages of plus strand RNA viruses[12, 13, 44]. Arteriviruses contain an array of two to four of these enzymes in the N-terminal domain of their replicase (9, 58, 60). Distant homologs of these arterivirus domains are also found in the large nsp3 product of coronaviruses[2, 21, 76], and it has been postulated that, in the course of nidovirus evolution, these N-terminal papain-like protease domains may have been optimally suited for acquisition and integration of new functions into an expanding replicase[12]. In the case of coronaviruses, engineered deletions and mutations affecting the nsp1 to -3 region and its proteolytic processing by nsp3 accessory proteinases can induce a variety of effects, but, remarkably, a large number of such mutations are tolerated to a certain extent[6, 17, 18, 74]. Thus far, a strictly transcription-specific function, as documented here for EAV nsp1, has not been identified in the coronavirus system, suggesting that arterivirus evolution may have taken a unique turn, by first acquiring multiple accessory PCP-containing replicase subunits and subsequently evolving a key regulatory position for these proteins in the viral life cycle.

ACKNOWLEDGEMENTS

We are grateful to Erwin van den Born, Martijn van Hemert, Richard Molenkamp, Alexander Pasternak, Clara Posthuma, and Willy Spaan for helpful comments and suggestions. We thank Erwin van den Born and Nancy Beerens for assistance with RNA structure predictions.

M.A.T. and D.D.N. were supported by grants 348-003 and 700.52.306, respectively, from the Council for Chemical Sciences of The Netherlands Organization for Scientific Research (NWO-CW).

REFERENCES

1. **Ahlquist, P.** 2006. Parallels among positive-strand RNA viruses, reversetranscribing viruses and double-stranded RNA viruses. Nat. Rev. Microbiol. **4:**371–382.
2. **Baker, S. C., N. La Monica, C. K. Shieh, and M. M. C. Lai.** 1990. Murine coronavirus gene 1 polyprotein contains an autoproteolytic activity. Adv.Exp. Biol. Med. **276:**283–289.
3. **Ball, L. A.** 2001. Replication strategies of RNA viruses, 105–118. *In* D. M.Knipe and P. M. Howley (ed.), Fields virology. Lippincott, Williams &Wilkins, Philadelphia, PA.
4. **Bartlam, M., H. Yang, and Z. Rao.** 2005. Structural insights into SARS-coronavirus proteins. Curr. Opin. Struct. Biol. **6:**664–672.
5. **Brierley, I., and F. J. Dos Ramos.** 2006. Programmed ribosomal frameshifting in HIV-1 and the SARS-CoV. Virus Res. **119:**29–42.
6. **Brockway, S. M., and M. R. Denison.** 2005. Mutagenesis of the murine hepatitis virus nsp1-coding region identifies residues important for protein processing, viral RNA synthesis, and viral replication. Virology **340:**209–223.
7. **Buck, K. W.** 1996. Comparison of the replication of positive-stranded RNA viruses of plants and animals. Adv. Virus Res. **47:**159–251.
8. **Dannull, J., A. Surovoy, G. Jung, and K. Moelling.** 1994. Specific binding of HIV-1 nucleocapsid protein to PSI RNA *in vitro* requires N-terminal zinc finger and flanking basic amino acid residues. EMBO J. **13:**1525–1533.
9. **den Boon, J. A., K. S. Faaberg, J. J. M. Meulenberg, A. L. M. Wassenaar, P. G. W. Plagemann, A. E. Gorbalenya, and E. J. Snijder.** 1995. Processing and evolution of the N-terminal region of the arterivirus replicase ORF1a protein: identification of two papainlike cysteine proteases. J. Virol. **69:**4500–4505.
10. **Dougherty, W. G., and B. L. Semler.** 1993. Expression of virus-encoded proteinases: functional and structural similarities with cellular enzymes. Microbiol. Rev. **57:**781–822.
11. **Gorbalenya, A. E.** 2001. Big nidovirus genome: when count and order of domains matter. Adv. Exp. Biol. Med. **494:**1–17.
12. **Gorbalenya, A. E., L. Enjuanes, J. Ziebuhr, and E. J. Snijder.** 2006. Nidovirales: evolving the largest RNA virus genome. Virus Res. **117:**17–37.
13. **Gorbalenya, A. E., E. V. Koonin, and M. M. C. Lai.** 1991. Putative papain-related thiol proteases of positive-strand RNA viruses. Identification of rubiand aphthovirus proteases and delineation of a novel conserved domain associated with proteases of rubi-, alpha- and coronaviruses. FEBS Lett. **288:**201–205.
14. **Gorbalenya, A. E., and E. J. Snijder.** 1996. Viral cysteine proteases. Persp. Drug Discov. Design. **6:**64–86.
15. **Gorelick, R. J., D. J. Chabot, D. E. Ott, T. D. Gagliardi, A. Rein, L. E. Henderson, and L. O. Arthur.** 1996. Genetic analysis of the zinc finger in the Moloney murine leukemia virus nucleocapsid domain: replacement of zinc-coordinating residues with other zinc-coordinating residues yields noninfectious particles containing genomic RNA. J. Virol. **70:**2593–2597.
16. **Gorelick, R. J., T. D. Gagliardi, W. J. Bosche, T. A. Wiltrout, L. V. Coren, D. J. Chabot, J. D. Lifson, L. E. Henderson, and L. O. Arthur.** 1999. Conservation of the retroviral nucleocapsid protein zinc finger is strongly influenced by its role in viral infection processes: characterization of HIV-1 particles containing mutant nucleocapsid zinc-coordinating sequences. Virology **256:**92–104.
17. **Graham, R. L., and M. R. Denison.** 2006. Replication of murine hepatitis virus is regulated by papain-like proteinase 1 processing of nonstructural proteins 1, 2, and 3. J. Virol. **80:**11610–11620.

18. **Graham, R. L., A. C. Sims, S. M. Brockway, R. S. Baric, and M. R. Denison.** 2005. The nsp2 replicase proteins of murine hepatitis virus and severe acute respiratory syndrome coronavirus are dispensable for viral replication. J. Virol. **79:**13399–13411.

19. **Gultyaev, A. P., F. H. van Batenburg, and C. W. Pleij.** 1995. The computer simulation of RNA folding pathways using a genetic algorithm. J. Mol. Biol. **250:**37–51.

20. **Guo, J., T. Wu, J. Anderson, B. F. Kane, D. G. Johnson, R. J. Gorelick, L. E. Henderson, and J. G. Levin.** 2000. Zinc finger structures in the human immunodeficiency virus type 1 nucleocapsid protein facilitate efficient minus- and plus-strand transfer. J. Virol. **74:**8980–8988.

21. **Harcourt, B. H., D. Jukneliene, A. Kanjanahaluethai, J. Bechill, K. M. Severson, C. M. Smith, P. A. Rota, and S. C. Baker.** 2004. Identification of severe acute respiratory syndrome coronavirus replicase products and characterization of papain-like protease activity. J. Virol. **78:**13600–13612.

22. **Kim, J. L., K. A. Morgenstern, C. Lin, T. Fox, M. D. Dwyer, J. A. Landro, S. P. Chambers, W. Markland, C. A. Lepre, E. T. O'Malley, S. L. Harbeson, C. M. Rice, M. A. Murcko, P. R. Caron, and J. A. Thomson.** 1996. Crystal structure of the hepatitis C virus NS3 protease domain complexed with a synthetic NS4A cofactor peptide. Cell **87:**343–355.

23. **Kummerer, B. M., and C. M. Rice.** 2002. Mutations in the yellow fever virus nonstructural protein NS2A selectively block production of infectious particles. J. Virol. **76:**4773–4784.

24. **Laity, J. H., B. M. Lee, and P. E. Wright.** 2001. Zinc finger proteins: new insights into structural and functional diversity. Curr. Opin. Struct. Biol. **11:**39–46.

25. **Landt, O., H.-P. Grunert, and U. Hahn.** 1990. A general method for rapid site-directed mutagenesis using the polymerase chain reaction. Gene **96:**125–128.

26. **Lee, N., R. J. Gorelick, and K. Musier-Forsyth.** 2003. Zinc finger-dependent HIV-1 nucleocapsid protein-TAR RNA interactions. Nucleic Acids Res. **31:**4847–4855.

27. **Liew, C. K., R. J. Y. Simpson, A. H. Y. Kwan, L. A. Crofts, F. E. Loughlin, J. M. Matthews, M. Crossley, and J. P. Mackay.** 2005. Zinc fingers as protein recognition motifs: structural basis for the GATA-1/Friend of GATA interaction. Proc. Natl. Acad. Sci. USA **102:**583–588.

28. **Lu, D., M. Alexandra Searles, and A. Klug.** 2003. Crystal structure of a zinc-finger-RNA complex reveals two modes of molecular recognition. Nature **426:**96–100.

29. **Maclachlan, N. J., U. B. Balasuriya, J. F. Hedges, T. M. Schweidler, W. H. McCollum, P. J. Timoney, P. J. Hullinger, and J. F. Patton.** 1998. Serologic response of horses to the structural proteins of equine arteritis virus. J. Vet. Diagn. Investig. **10:**229–236.

30. **Matthews, J. M., K. Kowalski, C. K. Liew, B. K. Sharpe, A. H. Fox, M. Crossley, and J. P. Mackay.** 2000. A class of zinc fingers involved in protein-protein interactions: biophysical characterization of CCHC fingers from Fog and U-shaped. Eur. J. Biochem. **267:**1030–1038.

31. **McCarty, A. S., G. Kleiger, D. Eisenberg, and S. T. Smale.** 2003. Selective dimerization of a C2H2 zinc finger subfamily. Mol. Cell **11:**459–470.

32. **Mesters, J. R., J. Tan, and R. Hilgenfeld.** 2006. Viral enzymes. Curr. Opin. Struct. Biol. **16:**776–786.

33. **Miller, J., A. D. McLachlan, and A. Klug.** 1985. Repetitive zinc-binding domains in the protein transcription factor Iiia from Xenopus oocytes. EMBO J. **4:**1609–1614.

34. **Miller, W. A., and G. Koev.** 2000. Synthesis of subgenomic RNAs by positive-strand RNA viruses. Virology **273:**1–8.

35. **Molenkamp, R., B. C. D. Rozier, S. Greve, W. J. M. Spaan, and E. J. Snijder.** 2000. Isolation and characterization of an arterivirus defective interfering RNA genome. J. Virol. **74:**3156–3165.

36. **Molenkamp, R., H. van Tol, B. C. D. Rozier, Y. van der Meer, W. J. M. Spaan, and E. J. Snijder.** 2000. The arterivirus replicase is the only viral protein required for genome replication and subgenomic mRNA transcription. J. Gen. Virol. **81:**2491–2496.

37. **Newman, J. F., P. G. Piatti, B. M. Gorman, T. G. Burrage, M. D. Ryan, M. Flint, and F. Brown.** 1994. Foot-and-mouth disease virus particles contain replicase protein 3D. Proc. Natl. Acad. Sci. USA **91:**733–737.
38. **Pasternak, A. O., W. J. M. Spaan, and E. J. Snijder.** 2004. Regulation of relative abundance of arterivirus subgenomic rnRNAs. J. Virol. **78:**8102–8113.
39. **Pasternak, A. O., W. J. M. Spaan, and E. J. Snijder.** 2006. Nidovirus transcription: how to make sense…? J. Gen. Virol. **87:**1403–1421.
40. **Pasternak, A. O., E. van den Born, W. J. M. Spaan, and E. J. Snijder.** 2001. Sequence requirements for RNA strand transfer during nidovirus discontinuous subgenomic RNA synthesis. EMBO J. **20:**7220–7228.
41. **Pasternak, A. O., E. van den Born, W. J. M. Spaan, and E. J. Snijder.** 2003. The stability of the duplex between sense and antisense transcription-regulating sequences is a crucial factor in arterivirus subgenomic mRNA synthesis. J. Virol. **77:**1175–1183.
42. **Paul, A. V., J. H. van Boom, D. Filippov, and E. Wimmer.** 1998. Protein-primed RNA synthesis by purified poliovirus RNA polymerase. Nature **393:** 280–284.
43. **Pedersen, K. W., Y. van der Meer, N. Roos, and E. J. Snijder.** 1999. Open reading frame 1a-encoded subunits of the arterivirus replicase induce endoplasmic reticulum-derived double-membrane vesicles which carry the viral replication complex. J. Virol. **73:**2016–2026.
44. **Peng, C.-W., A. J. Napuli, and V. V. Dolja.** 2003. Leader proteinase of *Beet yellows virus* functions in long-distance transport. J. Virol. **77:**2843–2849.
45. **Posthuma, C. C., D. D. Nedialkova, J. C. Zevenhoven-Dobbe, J. H. Blokhuis, A. E. Gorbalenya, and E. J. Snijder.** 2006. Site-directed mutagenesis of the nidovirus replicative endoribonuclease NendoU exerts pleiotropic effects on the arterivirus life cycle. J. Virol. **80:**1653–1661.
46. **Puustinen, P., M. L. Rajamaki, K. I. Ivanov, J. P. T. Valkonen, and K. Makinen.** 2002. Detection of the potyviral genome-linked protein VPg in virions and its phosphorylation by host kinases. J. Virol. **76:**12703–12711.
47. **Ramboarina, S., N. Moreller, M. C. Fournie-Zaluski, and B. P. Roques.** 1999. Structural investigation on the requirement of CCHH zinc finger type in nucleocapsid protein of human immunodeficiency virus 1. Biochemistry **38:**9600–9607.
48. **Sawicki, S. G., and D. L. Sawicki.** 1995. Coronaviruses use discontinuous extension for synthesis of subgenome-length negative strands. Adv. Exp. Biol. Med. **380:**499–506.
49. **Sawicki, S. G., and D. L. Sawicki.** 2005. Coronavirus transcription: a perspective, p. 31–55. *In* L. Enjuanes (ed.), Coronavirus replication and reverse genetics. Springer, Berlin, Germany.
50. **Sawicki, S. G., D. L. Sawicki, and S. G. Siddell.** 2007. A contemporary view of coronavirus transcription. J. Virol. **81:**20–29.
51. **Seybert, A., C. C. Posthuma, L. C. van Dinten, E. J. Snijder, A. E. Gorbalenya, and J. Ziebuhr.** 2005. A complex zinc finger controls the enzymatic activities of nidovirus helicases. J. Virol. **79:**696–704.
52. **Siddell, S. G., J. Ziebuhr, and E. J. Snijder.** 2005. Coronaviruses, toroviruses, and arteriviruses, p. 823–856. *In* B. W. Mahy and V. ter Meulen, Topley and Wilson's microbiology and microbial infections: virology volume. Hodder Arnold, London, United Kingdom.
53. **Snijder, E. J., P. J. Bredenbeek, J. C. Dobbe, V. Thiel, J. Ziebuhr, L. L. M. Poon, Y. Guan, M. Rozanov, W. J. M. Spaan, and A. E. Gorbalenya.** 2003. Unique and conserved features of genome and proteome of SARS-coronavirus, an early split-off from the coronavirus group 2 lineage. J. Mol. Biol. **331:**991–1004.
54. **Snijder, E. J., and J. J. M. Meulenberg.** 1998. The molecular biology of arteriviruses. J. Gen. Virol. **79:**961–979.

55. **Snijder, E. J., and J. J. M. Meulenberg.** 2001. Arteriviruses, p. 1205–1220. *In* D. M. Knipe and P. M. Howley, Fields virology. Lippincott, Williams & Wilkins, Philadelphia, PA.

56. **Snijder, E. J., S. G. Siddell, and A. E. Gorbalenya.** 2005. The order Nidovirales, p. 390–404. *In* B. W. Mahy and V. ter Meulen (ed.), Topley and Wilson's microbiology and microbial infections: virology volume. Hodder Arnold, London, United Kingdom.

57. **Snijder, E. J., H. van Tol, N. Roos, and K. W. Pedersen.** 2001. Non-structural proteins 2 and 3 interact to modify host cell membranes during the formation of the arterivirus replication complex. J. Gen. Virol. **82:**985–994.

58. **Snijder, E. J., A. L. M. Wassenaar, and W. J. M. Spaan.** 1992. The 5′ end of the equine arteritis virus replicase gene encodes a papainlike cysteine protease. J. Virol. **66:**7040–7048.

59. **Snijder, E. J., A. L. M. Wassenaar, and W. J. M. Spaan.** 1994. Proteolytic processing of the replicase ORF1a protein of equine arteritis virus. J. Virol. **68:**5755–5764.

60. **Snijder, E. J., A. L. M. Wassenaar, W. J. M. Spaan, and A. E. Gorbalenya.** 1995. The arterivirus nsp2 protease: an unusual cysteine protease with primary structure similarities to both papain-like and chymotrypsin-like proteases. J. Biol. Chem. **270:**16671–16676.

61. **Stote, R. H., E. Kellenberger, H. Muller, E. Bombarda, B. P. Roques, B. Kieffer, and Y. Mely.** 2004. Structure of the His44Ala single point mutant of the distal finger motif of HIV-1 nucleocapsid protein: a combined NMR, molecular dynamics simulation, and fluorescence study. Biochemistry **43:** 7687–7697.

62. **Tijms, M. A., L. C. van Dinten, A. E. Gorbalenya, and E. J. Snijder.** 2001. A zinc finger-containing papain-like protease couples subgenomic mRNA synthesis to genome translation in a positive-stranded RNA virus. Proc. Natl. Acad. Sci. USA **98:**1889–1894.

63. **van Aken, D., J. C. Zevenhoven-Dobbe, A. E. Gorbalenya, and E. J. Snijder.** 2006. Proteolytic maturation of replicase polyprotein pp1a by the nsp4 main proteinase is essential for equine arteritis virus replication and includes internal cleavage of nsp7. J. Gen. Virol. **87:**3473–3482.

64. **van den Born, E., A. P. Gultyaev, and E. J. Snijder.** 2004. Secondary structure and function of the 5′-proximal region of the equine arteritis virus RNA genome. RNA **10:**424–437.

65. **van den Born, E., C. C. Posthuma, A. P. Gultyaev, and E. J. Snijder.** 2005. Discontinuous subgenomic RNA synthesis in arteriviruses is guided by an RNA hairpin structure located in the genomic leader region. J. Virol. **79:** 6312–6324.

66. **van den Born, E., C. C. Posthuma, K. Knoops, and E. J. Snijder.** 2007. An infectious recombinant equine arteritis virus expressing green fluorescent protein from its replicase gene. J. Gen. Virol. **88:**1196–1205.

67. **van der Meer, Y., H. van Tol, J. Krijnse Locker, and E. J. Snijder.** 1998. ORF1a-encoded replicase subunits are involved in the membrane association of the arterivirus replication complex. J. Virol. **72:**6689–6698.

68. **van Dinten, L. C., J. A. den Boon, A. L. M. Wassenaar, W. J. M. Spaan, and E. J. Snijder.** 1997. An infectious arterivirus cDNA clone: identification of a replicase point mutation which abolishes discontinuous mRNA transcription. Proc. Natl. Acad. Sci. USA **94:**991–996.

69. **van Dinten, L. C., H. van Tol, A. E. Gorbalenya, and E. J. Snijder.** 2000. The predicted metal-binding region of the arterivirus helicase protein is involved in subgenomic mRNA synthesis, genome replication, and virion biogenesis. J. Virol. **74:**5213–5223.

70. **van Marle, G., J. C. Dobbe, A. P. Gultyaev, W. Luytjes, W. J. M. Spaan, and E. J. Snijder.** 1999. Arterivirus discontinuous mRNA transcription is guided by base-pairing between sense and antisense transcription-regulating sequences. Proc. Natl. Acad. Sci. USA **96:**12056–12061.

71. **Wieringa, R., A. A. F. de Vries, J. van der Meulen, G.-J. Godeke, J. J. M. Onderwater, H. van Tol, H. K. Koerten, A. M. Mommaas, E. J. Snijder, and P. J. M. Rottier.** 2004. Structural protein requirements in equine arteritis virus assembly. J. Virol. **78:**13019–13027.
72. **Zevenhoven-Dobbe, J. C., S. Greve, H. van Tol, W. J. M. Spaan, and E. J. Snijder.** 2004. Rescue of disabled infectious single-cycle (DISC) equine arteritis virus by using complementing cell lines that express minor structural glycoproteins. J. Gen. Virol. **85:**3709–3714.
73. **Ziebuhr, J.** 2004. Molecular biology of severe acute respiratory syndrome coronavirus. Curr. Opin. Microbiol. **7:**412–419.
74. **Ziebuhr, J., B. Schelle, N. Karl, E. Minskaia, S. Bayer, S. G. Siddell, A. E. Gorbalenya, and V. Thiel.** 2007. Human coronavirus 229E papain-like proteases have overlapping specificities but distinct functions in viral replication. J. Virol. **81:**3922–3932.
75. **Ziebuhr, J., E. J. Snijder, and A. E. Gorbalenya.** 2000. Virus-encoded proteinases and proteolytic processing in the *Nidovirales*. J. Gen. Virol. **81:**853–879.
76. **Ziebuhr, J., V. Thiel, and A. E. Gorbalenya.** 2001. The autocatalytic release of a putative RNA virus transcription factor from its polyprotein precursor involves two paralogous papain-like proteases that cleave the same peptide bond. J. Biol. Chem. **276:**33220–33232.
77. **Zuker, M.** 1989. On finding all suboptimal foldings of an RNA molecule. Science **244:**48–52.
78. **Zuker, M.** 2003. Mfold web server for nucleic acid folding and hybridization prediction. Nucleic Acids Res. **31:**3406–3415.